

# Creating solitons by means of spin-orbit coupling

Boris A. Malomed

*Department of Physical Electronics, School of Electrical Engineering, Faculty of Engineering,  
and Center for Light-Matter Interaction, Tel Aviv University, Tel Aviv 69978, Israel*

(Dated: June 1, 2018)

This mini-review collects theoretical results predicting the creation of matter-wave solitons by the pseudo-spinor system of Gross-Pitaevskii equations (GPEs) with the self-attractive cubic nonlinearity and linear first-order-derivative terms accounting for the spin-orbit coupling (SOC). In one dimension (1D), the so predicted bright solitons are similar to their well-known counterparts supported by the GPE in the absence of SOC. Completely novel results were recently obtained for 2D and 3D systems: SOC suppresses the collapse instability of the multidimensional GPE, creating fully stable 2D ground-state solitons and metastable 3D ones of two types: *semi-vortices* (SVs), with vorticities  $m = 1$  in one spin component and  $m = 0$  in the other, and *mixed modes* (MMs), with  $m = 0$  and  $m = \pm 1$  present in both components. With the Galilean invariance broken by SOC, moving solitons exist up to a certain critical velocity, suffering delocalization above it. The newest result predicts stable 2D “quantum droplets” of the MM type in the presence of the Lee-Huang-Yang corrections to the GPE system, induced by quantum fluctuations around the mean-field states, in the case when the inter-component attraction dominates over the self-repulsion in each component

## I. INTRODUCTION

Atomic gases, cooled to temperatures below the threshold for the transition into a quantum degenerate state (in particular, Bose-Einstein condensates (BEC) in bosonic gases [1, 2]), find an important application as a testbed allowing simulation of various effects, which were originally known in complex forms in condensed-matter physics, and may be realized (or emulated) in a simple and clean form in ultracold quantum gases [3]. BEC also offers a way to reproduce diverse phenomena which were previously discovered in optics [4]. The latter possibility is essentially based on the similarity of the nonlinear Schrödinger equation (NLSE), which is the basic propagation equation in optics [5], and the Gross-Pitaevskii equation (GPE), which is a universal model for ultracold bosonic gases [1]. In the framework of the similarity, the same cubic nonlinearity, which represents the Kerr term in optics, represents collisional effects in atomic BEC.

In particular, a binary ultracold *bosonic* gas, whose two-component mean-field wave function is considered as a pseudo-spinor, may emulate spinor effects in the *fermionic* gas of electrons with spin  $1/2$ , even if the true bosonic spin is zero. In this vein, great attention has been drawn to the experimentally demonstrated [6] BEC-based emulation of the spin-orbit coupling (SOC) in semiconductors, i.e., the linear interaction between the electron’s momentum and its spin. In terms of the atomic gas, SOC is mapped into a linear interaction of the atoms’ momentum and the pseudospin [6]-[11]. The mapping makes it also possible to include the Zeeman splitting (ZS) between up- and down-states of the electron, which is an important aspect of the solid-state SOC, represented by an energy difference between the two components of the BEC binary wave function [12]. In semiconductors, two fundamental types of SOC are represented by the Dresselhaus [13] and Rashba [14] Hamiltonians, each one admitting the emulation in ultracold gases.

While majority of experimental works on the emulation of SOC were carried out in effectively one-dimensional (1D) settings, the realization of the SOC in the quasi-2D BEC was reported too [15], encouraging the consideration of SOC-supported modes in multidimensional geometries, such as 2D [16]-[21] and 3D [22] solitons, vortices [23]-[26], skyrmions [27], etc. A crucial role in the creation of these nonlinear modes belongs to the sign of the nonlinearity. Thus far, SOC was realized in the  $^{87}\text{Rb}$  gas with repulsive interactions. Nevertheless, in other bosonic species which admit the transition to the BEC, the sign can be switched to attraction, by means of the Feshbach resonance [28, 29]. In particular, the application of this method to the condensate of  $^7\text{Li}$  [30, 31] and  $^{85}\text{Rb}$  [32] atoms has made it possible the creation of effectively 1D solitons.

This mini-review is focused on recently studied schemes allowing the creation of solitons in binary BEC systems featuring SOC between the components. Such experimental results were not yet reported, but a number of theoretical predictions provide an incentive for the development of the experiment in this direction. While in the 1D setting the addition of SOC does not lead to qualitative changes of the previously studied soliton phenomenology, the predictions for the 2D and 3D geometries suggest possibilities of the realization of essentially novel effects. Arguably, the most noteworthy ones are unique possibilities to create absolutely stable 2D [16] and metastable 3D [22] solitons in the self-attractive BEC, in spite of the presence of the critical and supercritical collapse, driven in the 2D and 3D space, respectively, by the cubic self-attraction [33, 34] (peculiarities of the collapse in SOC systems were considered in [35]). For this reason, the creation of stable multidimensional optical and matter-wave solitons is a challenging problem,

which has drawn a great deal of interest, see reviews [4, 36] and [37, 38]. The above-mentioned recent results make an essential contribution towards the solution of this problem. In particular, the mini-review includes the newest addition to the topic [39], namely the prediction of stable SOC solitons in the effectively 2D setting stabilized, at arbitrarily large values of their norm, by beyond-the-mean-field corrections, *viz.*, the Lee-Huang-Yang (LHY) terms [40], which are generated by quantum fluctuations around the mean-field states. Recently, it had been predicted theoretically [41, 42] and demonstrated experimentally [43–45] that the LHY effect readily stabilizes two-component 3D solitons, in the form of “quantum droplets” (QDs), against the collapse (in the system which does not include SOC effects).

The rest of the mini-review is structured as follows: basic models of SOC systems are formulated in Section II, main results for 2D and 3D solitons are summarized in Section III, and the article is completed by Section IV.

## II. THE BASIC MODELS: SYSTEMS OF COUPLED GPES

The system of GPEs in the 2D space  $(x, y)$  for the pseudo-spinor (two-component) wave function  $(\phi_+, \phi_-)$ , which includes the self-attraction with the coefficient scaled to be 1, cross-attraction with relative strength  $\gamma > 0$ , linear SOC terms of the Rashba and Dresselhaus types with respective coefficients  $\lambda$  and  $\lambda_D$ , and ZS with strength  $\Omega > 0$ , is written as [8]–[11], [17]

$$i \frac{\partial \phi_+}{\partial t} = -\frac{1}{2} \nabla^2 \phi_+ - (|\phi_+|^2 + \gamma |\phi_-|^2) \phi_+ + \left( \lambda D^{[-]} \phi_- - i \lambda_D D^{[+]} \phi_- \right) - \Omega \phi_+, \quad (1)$$

$$i \frac{\partial \phi_-}{\partial t} = -\frac{1}{2} \nabla^2 \phi_- - (|\phi_-|^2 + \gamma |\phi_+|^2) \phi_- - \left( \lambda D^{[+]} \phi_+ + i \lambda_D D^{[-]} \phi_+ \right) + \Omega \phi_-, \quad (2)$$

with  $D^{[\pm]} \equiv \partial/\partial x \pm i\partial/\partial y$ . The GPE system conserves the Hamiltonian, momentum, and the total norm, which is proportional to the number of atoms in the condensate:

$$N = \iint (|\phi_+|^2 + |\phi_-|^2) dx dy \equiv N_+ + N_-. \quad (3)$$

In scaled equations (1) and (2) the unit length corresponds to distance  $\sim 1 \mu\text{m}$  and  $N = 1$  is tantamount to  $\simeq 3 \times 10^3$  atoms [17]. The spectrum of excitations generated by the linearized version of Eqs. (1) and (2), for  $\phi_{\pm} \sim \exp(i\mathbf{k} \cdot \mathbf{r} - i\mu_{\pm}t)$ , where  $\mathbf{k}$  is the wave vector, contains two branches [21]:

$$\mu_{\pm} = \frac{k^2}{2} \pm \sqrt{(\lambda^2 + \lambda_D^2)k^2 + 4\lambda\lambda_D k_x k_y + \Omega^2}. \quad (4)$$

Solitons may exist at values of  $\mu$  which are not covered by Eq. (4) with real wavenumbers, i.e., at

$$\begin{aligned} \mu < -\frac{1}{2} \left[ (|\lambda| + |\lambda_D|)^2 + \frac{\Omega^2}{(|\lambda| + |\lambda_D|)^2} \right], \quad \text{if } (|\lambda| + |\lambda_D|)^2 > |\Omega|, \\ \mu < -|\Omega|, \quad \text{if } (|\lambda| + |\lambda_D|)^2 < |\Omega|. \end{aligned} \quad (5)$$

The 3D model was addressed in [22], with SOC of the *Weyl type* [7]:

$$\begin{aligned} & \left[ i \frac{\partial}{\partial t} + \frac{1}{2} \nabla^2 + i \lambda \nabla \cdot \sigma \right. \\ & \left. + \begin{pmatrix} |\phi_+|^2 + \gamma |\phi_-|^2 & 0 \\ 0 & |\phi_-|^2 + \gamma |\phi_+|^2 \end{pmatrix} \right] \begin{pmatrix} \phi_+ \\ \phi_- \end{pmatrix} = 0, \end{aligned} \quad (6)$$

where  $\nabla$  is the 3D gradient,  $\lambda$  is the SOC coefficient, and  $\sigma = (\sigma_x, \sigma_y, \sigma_z)$  is the set of three Pauli matrices. Actually, the existence of metastable 3D solitons [22] is a generic fact, which is also valid for other particular forms of SOC.

LHY corrections to the mean-field theory are relevant in the case when the self-interaction of each component is repulsive, while the self-trapping of solitons is provided by attraction between the components [41]. The 2D reduction of the original 3D GPEs with LHY terms replaces Eqs. (1) and (2) by the system which contains nonlinear terms with a logarithmic factor [39, 42]:

$$\begin{aligned} i \frac{\partial \phi_+}{\partial t} &= -\frac{1}{2} \nabla^2 \phi_+ + \lambda D^{[-]} \phi_- + g(|\phi_+|^2 - |\phi_-|^2) \phi_+ + \frac{g^2}{4\pi} (|\phi_+|^2 + |\phi_-|^2) \ln (|\phi_+|^2 + |\phi_-|^2) \phi_+, \\ i \frac{\partial \phi_-}{\partial t} &= -\frac{1}{2} \nabla^2 \phi_- - \lambda D^{[+]} \phi_+ + g(|\phi_-|^2 - |\phi_+|^2) \phi_- + \frac{g^2}{4\pi} (|\phi_+|^2 + |\phi_-|^2) \ln (|\phi_+|^2 + |\phi_-|^2) \phi_-, \end{aligned} \quad (7)$$

where  $g > 0$  is nonlinearity strength, and only SOC of the Rashba type, with coefficient  $\lambda$ , is included.

### III. STABLE 2D AND 3D SOLITONS IN THE SOC SYSTEM: SEMI-VORTICES (SVS) AND MIXED MODES (MMS)

*Semi-vortices.* Basic results for 2D solitons stabilized by SOC are presented here, following works [16, 17] and [46], where technical details can be found. First, Eqs. (1) and (2) admit stationary solutions of the SV type (also called half-vortices [25]). In the absence of the Dresselhaus and ZS terms,  $\lambda_D = \Omega = 0$ , SVs are built as bound states of zero-vorticity ( $m_+ = 0$ ) and vortical ( $m_- = 1$ ) self-trapped components, as per the following exact ansatz, written in terms of polar coordinates  $(r, \theta)$ , with chemical potential  $\mu$ :

$$\phi_+(x, y, t) = e^{-i\mu t} f_1(r^2), \quad \phi_-(x, y, t) = e^{-i\mu t + i\theta} r f_2(r^2), \quad (8)$$

with functions  $f_{1,2}(r^2)$  obeying equations

$$\begin{aligned} \mu f_1 + 2 \left[ r^2 \frac{d^2 f_1}{d(r^2)^2} + \frac{df_1}{d(r^2)} \right] + (f_1^2 + \gamma r^2 f_2^2) f_1 - 2\lambda \left[ r^2 \frac{df_2}{d(r^2)} + f_2 \right] &= 0, \\ \mu f_2 + 2 \left[ r^2 \frac{d^2 f_2}{d(r^2)^2} + 2 \frac{df_2}{d(r^2)} \right] + (r^2 f_2^2 + \gamma f_1^2) f_2 + 2\lambda \frac{df_1}{d(r^2)} &= 0. \end{aligned} \quad (9)$$

Due to their symmetry, Eqs. (1) and (2) also give rise to a mode which is a counterpart of SV (8) with vorticities  $(m_+, m_-) = (0, 1)$  replaced by  $(m_+, m_-) = (-1, 0)$ . At  $\gamma \leq 1$ , SVs represent the ground state (GS) of the system, i.e., an absolute minimum of the energy possible for a given norm (see details below). The coexistence of SV (8) and its counterpart implies *degeneracy of the GS*, which is possible in nonlinear systems, unlike linear ones. Solitons are solutions to Eq. (9) localized at  $r \rightarrow \infty$  as  $\exp\left(\sqrt{-(2\mu + \lambda^2)}r\right)$ , which exist at  $\mu < -\lambda^2/2$ . In the general case, with  $\lambda_D, \Omega \neq 0$ , solitons exist in the range of  $\mu$  given by Eq. (5).

A typical example of stable SVs, found as a numerical solution of Eq. (9), is displayed in Fig. 1. Results for the SV family are summarized in Figs. 1(b,c), which display the chemical potential as a function of the norm. It is seen that the zero-vorticity component always carries a larger share of the total norm. The negative local slope of the  $\mu(N)$  curve in Fig. 1(b) implies that it satisfies the Vakhitov-Kolokolov (VK) criterion [33, 34, 47], which is a necessary, but not sufficient, condition for the stability of solitons supported by self-attractive nonlinearities. The SV family exists at  $N < N_{\max} \equiv N_T \approx 5.85$ , the latter value being the collapse threshold, i.e., the norm of the 2D *Townes solitons* (TSs) [48] generated by the single GPE in the absence of SOC. Indeed, Fig. 1(c) shows that the vortex component  $\phi_-$  vanishes in the limit of  $N \rightarrow N_T$  ( $\mu \rightarrow -\infty$ ), hence in this limit SV degenerates into the unstable single-component TS. At  $N > N_T$ , solitons do not exist, as the norm exceeding the threshold value gives rise to the collapse. On the other hand, there is no minimum value of  $N$  necessary for the existence of stable SVs.

It is relevant to mention that the fundamental reason for the instability of TSs in the usual 2D NLSE is the invariance of this equation with respect to a scaling transformation, due to which all TSs have a single value of the norm,  $N_T$ . The presence of the SOC terms in Eqs. (1) and (2) breaks the scaling invariance and lifts the norm degeneracy, pushing the soliton's norm to  $N < N_T$ . This makes the destabilization of the TSs by the collapse impossible, as it may only be initiated by  $N \geq N_T$ .

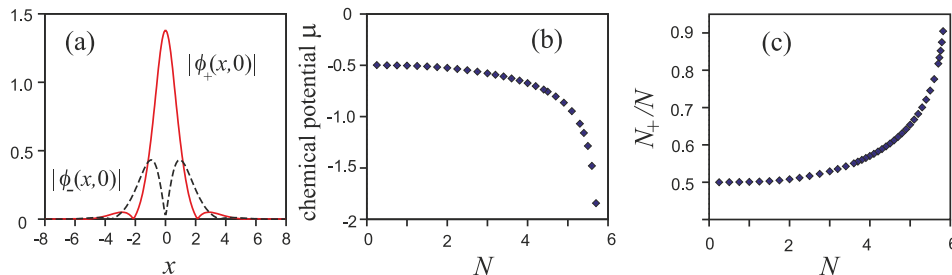


FIG. 1: (Color online) (a) Cross-sections of two components of the SV (semi-vortex),  $|\phi_+(x,0)|$  and  $|\phi_-(x,0)|$ , with norm  $N = 5$  and parameters  $\lambda = 1$ ,  $\gamma = \lambda_D = \Omega = 0$  in Eqs. (1) and (2). (b) and (c) Chemical potential  $\mu$  and the relative share of the norm in the zero-vorticity component,  $N_+/N$  (see Eq. (3)), vs.  $N$  for the SV family. The plots are borrowed from [16] and [46].

*Mixed modes.* Another type of 2D self-trapped vortical states supported by Eqs. (1) and (2) can be produced by input

$$(\phi_{\pm}^0)_{\text{MM}} = B_1 e^{-\beta_1 r^2} \mp B_2 r e^{\mp i\theta - \beta_2 r^2}, \quad (10)$$

with real constants  $B_{1,2}$  and  $\beta_{1,2} > 0$  (unlike the SV ansatz (8), this one is not compatible with the equations, being used only an initial guess, or a basis for the variational approximation [16]). Modes generated by this input are called MMs as they mix vorticities  $(0, -1)$  and  $(0, +1)$  in the two components, which have equal norms (unlike SV). A typical example of the stable MM and  $\mu(N)$  dependence for the MM family, which again satisfies the VK criterion, are displayed in Figs. 2(a) and (b), respectively (for the system without the Dresselhaus and ZS terms, i.e.,  $\lambda_D = \Omega = 0$ ). The norms of the two MM's components are always equal, while their maxima are separated by distance  $\Delta X$ , see Fig. 2(c). MMs exist at

$$N < N_{\text{max}} \equiv 2N_{\text{T}}/(1 + \gamma), \quad (11)$$

where  $N_{\text{T}}$  is the above-mentioned TS norm. In the limit of  $\mu \rightarrow -\infty$  ( $N \rightarrow N_{\text{max}}$ ), the vortex terms vanish in the MM, and it degenerates into an unstable two-component TS, similar to the above-mentioned degeneration of the SV. Other similarities are that  $N > N_{\text{max}}$  leads to the collapse, and, on the other hand, there is no minimum norm necessary for the existence of stable MMs.

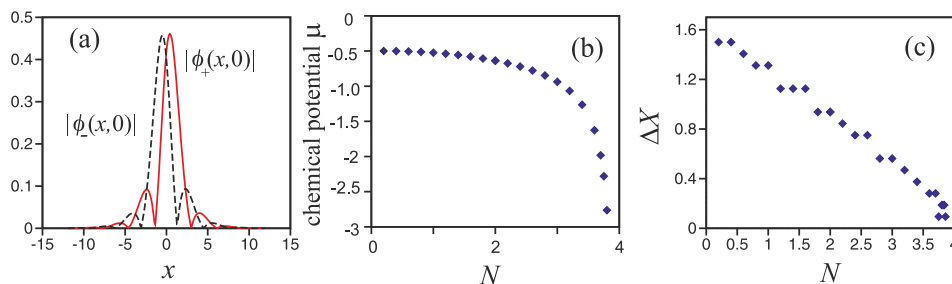


FIG. 2: (Color online) (a,b) The same as in Fig. 1 (a,b), but for stable MMs (mixed modes) at  $\gamma = 2$ . (c) Separation  $\Delta X$  between peak positions of  $|\phi_{+}(x,0)|^2$  and  $|\phi_{-}(x,0)|^2$  vs. the total norm. The plots are borrowed from [16] and [46].

While, as mentioned above, SV plays the role of GS at  $\gamma \leq 1$ , the MM represents GS at  $\gamma \geq 1$ . The *switch* between SV and MM at  $\gamma = 1$  is explained by comparison of values of the Hamiltonian for SV and MM at equal values of  $N$ , which shows that SV and MM realize the energy minimum at  $\gamma \leq 1$  and  $\gamma \geq 1$ , respectively. Accordingly, SV and MM are unstable, severally, at  $\gamma > 1$  and  $\gamma < 1$ : in these cases, SV starts spontaneous motion, while MM spontaneously breaks the symmetry between its two components, tending to rearrange itself into SV [16]. Furthermore, the analysis can be extended to  $\gamma < 0$  in Eqs. (1) and (2), i.e., to the system combining self-attraction and cross-repulsion of the two components, in which stable SVs exist as well [39]. In the same vein, one can consider the system with competing self-repulsion and cross-attraction, which maintains stable MMs [39].

In addition to the two fundamental species of the 2D solitons, SV and MM, Eqs. (1) and (2) give rise to excited states, obtained by adding vorticity  $M \geq 1$  to both components. In particular, the excited-state variety of SV is supplied by an exact ansatz which is a straightforward extension of (8), with  $\phi_{+}(x, y, t) = e^{-i\mu t + iM\theta} r^m f_1(r^2)$ ,  $\phi_{-}(x, y, t) = e^{-i\mu t + i(M+1)\theta} r^{m+1} f_2(r^2)$ , inputs generating excited states of MM being more complex. However, all the excited states, on the contrary to their fundamental counterparts, are completely unstable [16].

*Motion and collisions of SVs and MMs.* Generation of moving 2D solitons from the quiescent ones considered above is a nontrivial issue, because SOC terms break the Galilean invariance of Eqs. (1) and (2). In particular, the application of the formal Galilean transform for motion along the  $y$  axis with velocity  $v_y$ ,  $\phi_{\pm}(x, y, t) \equiv \tilde{\phi}_{\pm}(x, \tilde{y} \equiv y - v_y t, t) \exp(i v_y y - i v_y^2 t / 2)$ , casts Eqs. (1) and (2) with  $\lambda_D = \Omega = 0$  into the form differing from the original one by the presence of linear mixing terms with coefficient  $\lambda v_y$ :

$$\begin{aligned} i \frac{\partial \phi_{+}}{\partial t} &= -\frac{1}{2} \tilde{\nabla}^2 \phi_{+} - (|\phi_{+}|^2 + \gamma |\phi_{-}|^2) \phi_{+} + \lambda \tilde{D}^{[-]} \phi_{-} + \lambda v_y \phi_{-}, \\ i \frac{\partial \phi_{-}}{\partial t} &= -\frac{1}{2} \tilde{\nabla}^2 \phi_{-} - (|\phi_{-}|^2 + \gamma |\phi_{+}|^2) \phi_{-} - \lambda \tilde{D}^{[+]} \phi_{+} + \lambda v_y \phi_{+} \end{aligned} \quad (12)$$

(the tilde in Eq. (12) implies the replacement of  $\partial/\partial y$  by  $\partial/\partial \tilde{y}$ ). Stationary solutions to Eq. (12) are tantamount to steadily moving modes in the laboratory reference frame. It was thus found that Eqs. (1) and (2) with  $\lambda_D = \Omega = 0$

cannot generate moving solitons with  $v_x \neq 0$ , while MM can be set in the steady motion in the direction of  $y$ , with the velocity up to a certain maximum value,  $|v_y| < v_{\max}$ . Fixing the norm of the moving MM, one observes that its amplitude decays with the increase of  $v_y$ , vanishing at  $v_y = v_{\max}$ , i.e., the MM suffers delocalization at this point [16]. For instance,  $v_{\max} \approx 1.8$  for  $\lambda = 1$ ,  $\gamma = 2$  and  $N = 3.1$ . SV may also be set in motion along  $y$ , but its limit velocity is very small (roughly, smaller by a factor  $\sim 50$  in comparison with MMs). Finally, the availability of MMs moving with velocities  $\pm v_y$  makes it possible to simulate collisions between them, resulting in their fusion into a single mode, also of the MM type [16].

*Effect of combined Rashba and Dresselhaus SOC.* When the Dresselhaus terms, with  $\lambda_D \neq 0$ , are present in Eqs. (1) and (2), an exact ansatz similar to one (8) is not available, but a numerical SV solution can be constructed starting from initial guess  $\phi_+^{(0)}(x, y) = A_1 \exp(-\alpha_1 r^2)$ ,  $\phi_-^{(0)}(x, y) = A_2 e^{i\theta} r \exp(-\alpha_2 r^2)$ , with constants  $A_{1,2}$  and  $\alpha_{1,2} > 0$ , while a solution for MM is generated by the same ansatz (10) as above. As a result, it is found that, again, SV and MM realize GS at  $\gamma < 1$  and  $\gamma > 1$ , respectively [17].

The most essential effect caused by the inclusion of the Dresselhaus terms is destruction (delocalization) of SV and MM when  $\lambda_D$  exceeds certain critical values, which are growing functions of  $N$  and depend on  $\gamma$ . In other words, SV and MM exist in intervals, respectively,  $N_{\min}^{(\text{SV})}(\lambda_D) < N < N_T$  and  $N_{\min}^{(\text{MM})}(\lambda_D) < N < 2(1 + \gamma)^{-1} N_T$ , where  $N_T$  is, as above, the TS norm, cf. Eq. (11) [17]. These results are summarized in Fig. 3, which shows stability regions for SVs and MMs in the  $(N, \lambda_D)$  plane at  $\gamma = 0$  and  $\gamma = 2$ , respectively. The presence of the threshold value  $N_{\min}$  necessary for the existence of the solitons is a drastic difference from the system with  $\lambda_D = 0$ , cf. Figs. 1(b) and 2(b). On the other hand, it is easy to see that the upper limits,  $N_T$  and  $2(1 + \gamma)^{-1} N_T$ , do not depend on  $\lambda_D$ . Note that the critical values of the Dresselhaus coupling constant, up to which the solitons persist, are essentially larger for MM than for SV.

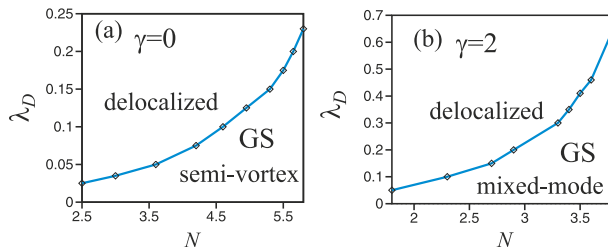


FIG. 3: (Color online) (a) and (b): Existence domains for the ground state in the form of SV (with  $\gamma = 0$ ) and MM ( $\gamma = 2$ ), respectively, in the plane of norm  $N$  and Dresselhaus coupling constant  $\lambda_D$ . Other parameters in Eqs. (1) and (2) are  $\lambda = 1$  and  $\Omega = 0$ . The plots are borrowed from [17] and [46].

*Effects of the Zeeman splitting (ZS).* Through the trend to populate one pseudo-spin component and depopulate the other one, the ZS essentially affects the SOC soliton phenomenology [17]. In particular, the stationary version of Eqs. (1) and (2), with  $\phi_{\pm} = e^{-i\mu t} u_{\pm}(x, y)$ , admits the application of a simple analytical approximation in the limit of large  $\Omega$ , setting  $\mu = -\Omega + \delta\mu$ , with  $|\delta\mu| \ll \Omega$ . In this limit, fixing  $\lambda = 1$  and  $\lambda_D = 0$ , one can eliminate the depopulated component in favor for the other one:  $u_- \approx (2\Omega)^{-1} D^{[+]} u_+$ , which obeys the stationary NLSE,  $(\delta\mu) u_+ = -(1/2) (1 - \Omega^{-1}) \nabla^2 u_+ - |u_+|^2 u_+$ . Up to rescaling, this NLSE gives rise to the zero-vorticity TS, while  $u_-$  is a small vortex component of the SV complex. With regard to the smallness of  $1/\Omega$ , the SV's norm is found, by means of the scaling argument, as

$$N = (1 - \Omega^{-1}) N_T + \mathcal{O}(\Omega^{-2}). \quad (13)$$

Thus, the norm is slightly smaller than the collapse threshold, keeping the SV protected against the collapse. The conclusion is that, at large  $\Omega$ , GS is of the SV type, irrespective of the value of the cross-attraction coefficient,  $\gamma$ , which does not appear in this approximation.

Because Eq. (13) produces only values of  $N$  close to  $N_T$  at large  $\Omega$ , one may expect that SVs with smaller norms suffer delocalization with the increase of  $\Omega$  at some critical value  $\Omega_{\text{cr}}$ . This is indeed demonstrated by both the variational approximation and numerical results [17], see Fig. 4(a) (for instance,  $\Omega_{\text{cr}}(\gamma = 0, N = 3) \approx 1.95$ ). In agreement with the above approximation, at  $\Omega < \Omega_{\text{cr}}$  stable SV keeps vorticity  $m = 1$  in the component with a smaller norm, and zero vorticity in the heavier component. As concerns MM, it is ousted by SV with the increase of  $\Omega$ . This is seen in the increase of the value of  $\gamma_{\text{cr}}$ , above which MM plays the role of GS: while, as mentioned above,  $\gamma_{\text{cr}} = 1$  is the universal SV-MM boundary at  $\Omega = 0$ , Fig. 4(b) demonstrates that  $\gamma_{\text{cr}}$  grows nearly linearly with the increase of  $\Omega$ . At  $\gamma > \gamma_{\text{cr}}$ , the symmetry between two MM's components, which holds at  $\Omega = 0$ , is broken, the norm of  $\phi_+$  being larger, with a progressively smaller vortex part in it.



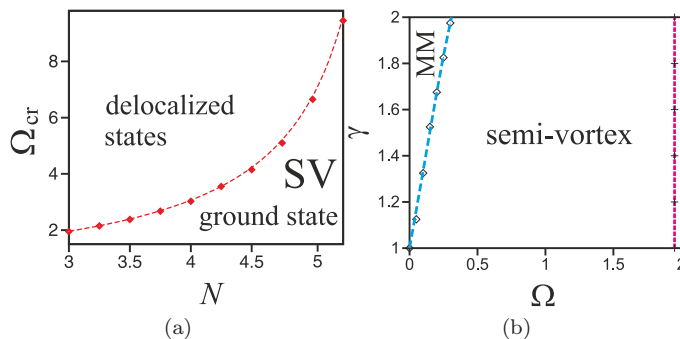


FIG. 4: (Color online) (a) The critical ZS strength,  $\Omega_{\text{cr}}$ , at which GS in the form of SV suffers delocalization, vs.  $N$ , for  $\lambda = 1$  and  $\gamma = \lambda_D = 0$  in Eqs. (1) and (2). (b) The numerically found boundary, in the  $(\Omega, \gamma)$  plane, for fixed  $N = 3$  and  $\lambda = 1$ ,  $\lambda_D = 0$ , between GSs of the MM and SV types. The vertical line corresponds to  $\Omega \approx 1.95$  at which the SV suffers the delocalization. The plots are borrowed from [17] and [46].

*Metastable 3D solitons.* As said above, in 2D the SOC system creates the otherwise missing GS at  $N < N_{\text{max}}$ , while inputs with  $N > N_{\text{max}}$  undergo the collapse. As shown in [22], SOC added to the 3D system (6) can never suppress the supercritical collapse, therefore the 3D system has no GS, which would realize an absolute minimum of the energy. Nevertheless, a variational analysis predicts metastable 3D solitons which represent a local energy minimum, i.e., such solitons are stable against small perturbations. Numerically, they can be produced by inputs similar to those adopted in the 2D system (see, e.g., Eq. (10)), with an extra factor  $\exp(-\gamma z^2)$  providing the localization in  $z$  for  $\gamma > 0$ . As a result, both the variational approximation and numerical analysis generate families of 3D metastable solitons, which are SV and MM at  $\gamma < 1$  and  $\gamma > 1$ , respectively, see examples in Fig. 5. Fixing  $\lambda = 1$  in Eq. (6), the conclusion is that, similar to the 2D setting (cf. Eq. (11)), the metastable 3D solitons exist at values of the 3D norm  $N_{3\text{D}} < (N_{3\text{D}})_{\text{max}}(\gamma)$ , the largest value being  $(N_{3\text{D}})_{\text{max}}(\gamma = 0) \approx 11.5$  [22].

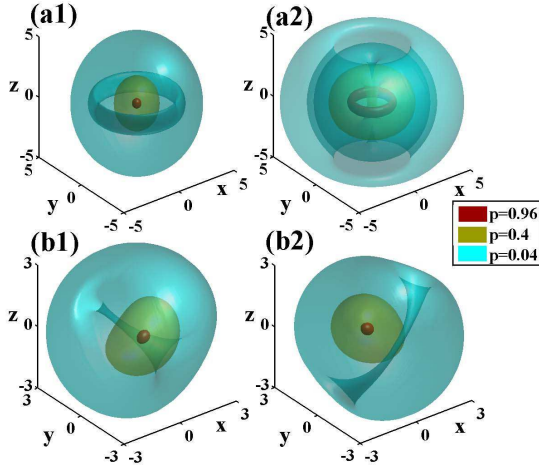


FIG. 5: (Color online) Density profiles of metastable 3D solitons with  $N_{3\text{D}} = 8$ , of the SV (a) and MM (b) types, generated by Eq. (6) with  $\lambda = 1$  and  $\gamma = 0.3$  in (a), or  $\gamma = 1.5$  in (b). The SV's zero-vorticity and vortex components,  $|\phi_+|$  and  $|\phi_-|$ , are plotted in (a1) and (a2), respectively, while the MM's components are shown in (b1) and (b2). In each panel, colors represent surfaces of fixed absolute values,  $|\phi_{\pm}| = p|\phi_{\pm}|_{\text{max}}$ , with  $p = 0.96, 0.40$ , and  $0.04$ . The plots are borrowed from [22].

*2D “quantum droplets” (QDs) of the MM type stabilized by the LHY corrections.* A general property of absolutely stable 2D solitons and metastable 3D ones is that they exist below a critical value of the norm, see, e.g., Eq. (11). On the other hand, as LHY terms may stabilize 3D and 2D solitons against the collapse, in the form of QDs [41, 42], the SOC system (7), including the LHY terms in their 2D form, gives rise to a family of stable QDs of the MM type, without any upper boundary  $N_{\text{max}}$ . As shown in Fig. 6, a characteristic feature of the SOC-affected QDs is their elongated shape, which may have arbitrary orientation in the  $(x, y)$  plane, due to the azimuthal invariance of Eqs. (6): if there is a stationary solution  $\{\phi_+(r, \theta), \phi_-(r, \theta)\}$ , its rotated version,  $\{\tilde{\phi}_+, \tilde{\phi}_-\} = \{\phi_+(r, \theta + \theta_0), e^{-i\theta_0} \phi_-(r, \theta + \theta_0)\}$ ,

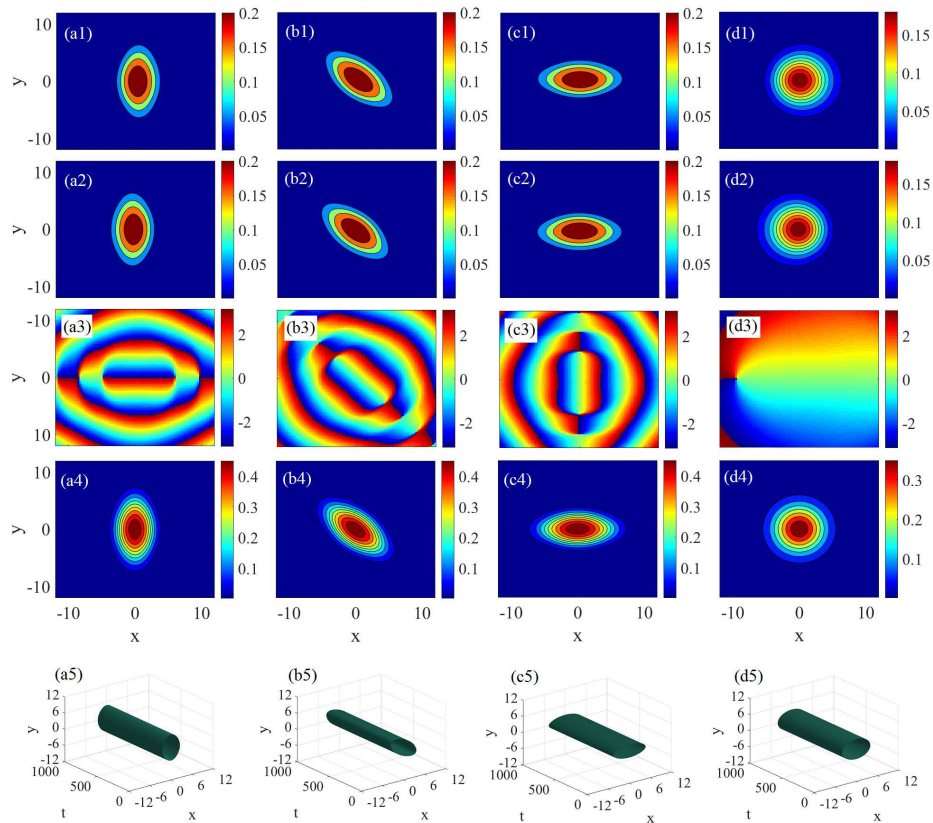


FIG. 6: (Color online) Typical examples of elongated QDs (“quantum droplets”), generated by Eq. (7) with  $(g, \lambda, N) = (2, 1, 20)$ , are displayed in columns (a-c), with the vertical, diagonal, and horizontal orientations, respectively. The first and second rows display density patterns  $|\phi_+(\mathbf{r})|^2$  and  $|\phi_-(\mathbf{r})|^2$ , the phase pattern of  $\phi_+$  is presented in the third row, the fourth row shows the total density profile,  $|\phi_+(\mathbf{r})|^2 + |\phi_-(\mathbf{r})|^2$ , and the fifth row illustrates the stability of the QDs in direct simulations of Eq. (7) (shown by the evolution of the total density). Column (d) is an example of QD with  $(g, \lambda, N) = (2, 0.2, 20)$ , which is nearly isotropic, as  $\lambda$  is small. The plots are borrowed from [39].

with arbitrary angle  $\theta_0$ , is a solution too [39]. Remarkably, all QDs are stable, as illustrated by plots in the bottom row of Fig. 6. Lastly, if SOC terms of both the Rashba and Dresselhaus types are included, Eq. (7) generates QDs for any ratio  $\lambda_D/\lambda$  of their strengths, including  $\lambda_D/\lambda = 1$ , while, in the absence of the LHY effect, MM exists only at essentially smaller values of  $\lambda_D/\lambda$ , see Fig. 3(b).

#### IV. CONCLUSION

This mini-review focuses on recently produced theoretical results which demonstrate the possibility of the creation of absolutely stable 2D [16, 17] and metastable 3D [22] solitons supported by SOC in binary BEC with attractive nonlinearity. The most essential prediction is that, on the contrary to the commonly known instability of 2D solitons and solitary vortices created by cubic self-attraction, two *stable* soliton species, SV (semi-vortex) and MM (mixed mode), are supported by SOC. In 2D, SV and MM represent the GS (ground state) when self-attraction in each component is, respectively, stronger or weaker than its cross-interaction counterpart. SV is made more favorable if ZS (Zeeman splitting) is applied. A broad class of stable MMs was recently predicted [39] in the 2D system which includes beyond-mean-field (LHY) corrections. These results suggest novel possibilities for the creation of stable vorticity-bearing solitons in BEC. An analog of SOC can also be implemented in optics, which was used to predict stable spatiotemporal solitons in nonlinear dual-core planar waveguides [21, 49].

The work can be extended in other directions. In particular, if SOC acts in a confined 2D or 3D spatial domain (similar to the 1D setting introduced in [50]), it is relevant to identify a minimum size of the domain which is sufficient for the creation of stable solitons. Further, it is interesting to construct 3D solitons in the SOC system which includes LHY terms, and to consider effects of ZS on 3D solitons. It may also be relevant to apply the concept of the

“nonlinearity management” [51] to the SOC system, periodically switching it, by means of time-dependent Feshbach resonance, between settings in which SV and MM represent GS.

*Acknowledgments.* I appreciate valuable collaborations with H. Sakaguchi, B. Li, E. Ya. Sherman, and Y. Li, which have produced results surveyed in this mini-review. I thanks G. Muga for the invitation to write this article. My work on the topic is partly supported by Israel Science Foundation, project No. 1287/17.

- 
- [1] L. P. Pitaevskii and S. Stringari, *Bose-Einstein Condensation*, Oxford University Press, Oxford, 2003.
- [2] V. S. Bagnato, D. J. Frantzeskakis, P. G. Kevrekidis, B. A. Malomed, and D. Mihalache, *Rom. Rep. Phys.* **67**, 5 (2015).
- [3] P. Hauke, F. M. Cucchietti, L. Tagliacozzo, I. Deutsch, and M. Lewenstein, *Rep. Prog. Phys.* **75**, 082401 (2012).
- [4] B. Malomed, L. Torner, F. Wise, and D. Mihalache, *J. Phys. B: At. Mol. Opt. Phys.* **49**, 170502 (2016).
- [5] Y. S. Kivshar and G. P. Agrawal, *Optical Solitons: From Fibers to Photonic Crystals* (Academic Press, San Diego, 2003).
- [6] Y. J. Lin, K. Jimenez-Garcia, and I. B. Spielman, *Nature* **471**, 83 (2011).
- [7] B. M. Anderson, G. Juzeliūnas, V. M. Galitski, and I. B. Spielman, *Phys. Rev. Lett.* **108**, 235301 (2012).
- [8] I. B. Spielman, *Ann. Rev. Cold At. Mol.* **1**, 145 (2012).
- [9] V. Galitski and I. B. Spielman, *Nature* **494**, 49 (2013).
- [10] N. Goldman, G. Juzeliūnas, P. Öhberg, and I. B. Spielman, *Rep. Progr. Phys.* **77**, 126401 (2014).
- [11] H. Zhai, *Rep. Prog. Phys.* **78**, 026001 (2015).
- [12] D. L. Campbell, G. Juzeliūnas, and I. B. Spielman, *Phys. Rev. A* **84**, 025602 (2011).
- [13] G. Dresselhaus, *Phys. Rev.* **100**, 580 (1955).
- [14] Y. A. Bychkov and E. I. Rashba, *J. Phys. C* **17**, 6039 (1984).
- [15] Z. Wu, L. Zhang, W. Sun, X.-T. Xu, B.-Z. Wang, S.-C. Ji, Y. Deng, S. Chen, X.-J. Liu, and J.-W. Pan, *Science* **354**, 83 (2016).
- [16] H. Sakaguchi, B. Li, and B. A. Malomed, *Phys. Rev. E* **89**, 032920 (2014).
- [17] H. Sakaguchi, E. Ya. Sherman, and B. A. Malomed, *Phys. Rev. E* **94**, 032202 (2016).
- [18] H. Sakaguchi and B. A. Malomed, *Phys. Rev. E* **90**, 062922 (2014).
- [19] L. Salasnich, W. B. Cardoso, and B. A. Malomed, *Phys. Rev. A* **90**, 033629 (2014).
- [20] V. E. Lobanov, Y. V. Kartashov, and V. V. Konotop, *Phys. Rev. Lett.* **112**, 180403 (2014).
- [21] H. Sakaguchi and B.A. Malomed, *New J. Phys.* **18**, 105005 (2016).
- [22] Y.-C. Zhang, Z.-W. Zhou, B. A. Malomed, and H. Pu, *Phys. Rev. Lett.* **115**, 253902 (2015).
- [23] T. Kawakami, T. Mizushima, and K. Machida, *Phys. Rev. A* **84**, 011607 (2011).
- [24] H. Sakaguchi and B. Li, *Phys. Rev. A* **87**, 015602 (2013).
- [25] B. Ramachandhran, B. Opanchuk, X.-J. Liu, H. Pu, P. D. Drummond, and H. Hu, *Phys. Rev. A* **85**, 023606 (2012).
- [26] A. L. Fetter, *Rev. Mod. Phys.* **81**, 647 (2009).
- [27] T. Kawakami, T. Mizushima, M. Nitta, and K. Machida, *Phys. Rev. Lett.* **109**, 015301 (2012).
- [28] S. L. Cornish, N. R. Claussen, J. L. Roberts, E. A. Cornell, and C. E. Wieman, *Phys. Rev. Lett.* **85**, 1795 (2000).
- [29] C. Chin, R. Grimm, P. Julienne, and E. Tiesinga, *Rev. Mod. Phys.* **82**, 1225 (2010).
- [30] K. E. Strecker, G. B. Partridge, A. G. Truscott, and R. G. Hulet, *Nature* **417**, 150 (2002).
- [31] L. Khaykovich, F. Schreck, G. Ferrari, T. Bourdel, J. Cubizolles, L. D. Carr, Y. Castin, and C. Salomon, *Science* **296**, 1290 (2002).
- [32] S. L. Cornish, S. T. Thompson, and C. E. Wieman, *Phys. Rev. Lett.* **96**, 170401 (2006).
- [33] L. Bergé, *Phys. Rep.* **303**, 259 (1998).
- [34] G. Fibich, *The Nonlinear Schrödinger Equation: Singular Solutions and Optical Collapse* (Springer: Heidelberg, 2015).
- [35] Sh. Mardonov, E. Ya. Sherman, J. G. Muga, H.-W. Wang, Y. Ban, and X. Chen, *Phys. Rev. A* **91**, 043604 (2015).
- [36] B. A. Malomed, D. Mihalache, F. Wise, and L. Torner, *J. Optics B: Quant. Semicl. Opt.* **7**, R53 (2005).
- [37] B. A. Malomed, *Eur. Phys. J. Special Topics* **225**, 2507 (2016).
- [38] D. Mihalache, *Rom. Rep. Phys.* **69**, 403 (2017).
- [39] Y. Li, Z. Luo, Y. Liu, Z. Chen, C. Huang, S. Fu, H. Tan, and B. A. Malomed, *New. J. Phys.* **19**, 113043 (2017).
- [40] T. D. Lee, K. Huang, and C. N. Yang, *Phys. Rev.* **106**, 1135 (1957).
- [41] D. S. Petrov, *Phys. Rev. Lett.* **115**, 155302 (2015).
- [42] D. S. Petrov and G. E. Astrakharchik, *Phys. Rev. Lett.* **117**, 100401 (2016).
- [43] C. R. Cabrera, L. Tanzi, J. Sanz, B. Naylor, P. Thomas, P. Cheiney, and L. Tarruell, *Science* **359**, 301 (2018)
- [44] P. Cheiney, C. R. Cabrera, J. Sanz, B. Naylor, L. Tanzi, and L. Tarruell, *Phys. Rev. Lett.* **120**, 135301 (2018).
- [45] G. Semeghini, G. Ferioli, L. Masi, C. Mazzinghi, L. Wolswijk, F. Minardi, M. Modugno, G. Modugno, M. Inguscio, and M. Fattori, arXiv:1710.10890.
- [46] H. Sakaguchi, B. Li, E. Ya. Sherman, and B. A. Malomed, *Romanian Rep. Phys.* **70**, 502 (2018).
- [47] M. Vakhitov and A. Kolokolov, *Radiophys. Quant. Electron.* **16**, 783 (1973).
- [48] R. Y. Chiao, E. Garmire, and C. H. Townes, *Phys. Rev. Lett.* **13**, 479 (1964).
- [49] Y. V. Kartashov, B. A. Malomed, V. V. Konotop, V. E. Lobanov, and L. Torner, *Opt. Lett.* **40**, 1045 (2015).
- [50] Y. V. Kartashov, V. V. Konotop, and D. A. Zezyulin, *Phys. Rev. A* **90**, 063621 (2014).
- [51] B. A. Malomed, *Soliton Management in Periodic Systems* (Springer: New York, 2006).